ISSN 1392 - 1207. MECHANIKA. 2010. Nr.5(85)

Time-frequency analysis of the current measurement by hall effect sensors for electric arc welding machine

T.Ç. Akıncı

Kirklareli University, Technical Education Faculty, Department of Electrical Education, 39060, Kirklareli, Turkey, E-mail: cetinakinci@kirklareli.edu.tr

1. Introduction

An electric arc that forms by a welding power source can be considered as a transformation of electrical energy to heat energy which is required during the arc welding. The arc welding involves low-voltage, high current arcs between the electrode and material as a work piece [1].

Some important applications of the electric arcs in which it is desirable to know the arc parameters accurately are in arc welding, plasma torches, switchgear, and arc furnaces [2, 3].

All electric welding machines perform the same function regardless of their size; they melt pieces of metal in order to mechanically bond them together [4-8].

They output a low voltage alternating current called AC at a high amperage. The voltage range is between 24 and 50 volts AC while the current value changes from 20 amperes to as high as 500 amperes. The effect of this high current appears as a blue arc in welding. This arc at high temperature heats up the metal and then it melts a puddle of molten metal.

The most common welder used in industrial is the arc welder. This type of electric machine uses a stick electrode to conduct the electricity to sample material and hence it melts at the same time to fill in the gaps. A wire feed machine uses a roll of wire and the wire feeds into the blue arc and fills in the gap between the two pieces of metal. A Tungsten Inert Gas (TIG) machine or welder uses a tungsten tip which creates the high temperature needed in the welding process. Along with the arc, an inert gas such as argon is fed into the TIG welding puddle of metal to remove any impurities that come from the surrounding environment [6].

In recent years, a great deal of the research on spectra of welding plasma has been undertaken considering the acquisition of spectrum signal and practical applications in monitoring the welding quality [9, 10].

In this study, spectral properties of the current signals of electric arc welding machine are examined under the time-frequency analysis methods. Hence the current variations related to the welding machine are detailed using the spectral approaches like spectrograms and Power Spectral Analysis (PSD) method.

2. Hall effect current measurement

In this study, the measurement of the primer current drawn by the welter is realized with the help of a linear Hall-effect sensor. The sensor should be placed at an air gap which is formed over the coil in order to detect the current. Primer coil may be composed of multiple turns as well as it can be used as only one winding (conductive element carrying the current directly passes through coil) (Fig. 1) too. Due to Hall-effect magnetic flux generated by primer current in toroid produces voltage proportional to the flux density at the ends of the sensor [11-13].

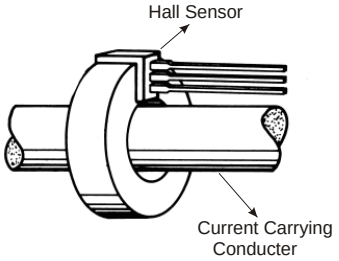

Fig. 1 Current measurement with Hall-effect sensor [12]

In this study, linear Hall-effect sensor of A3516 Allegro Company is preferred. A3516 has a sensitivity of $2.5\ 10^4$ mV/T (2.5 mV/G). Operational voltage interval of the sensor is between 4.5 V and 5.5 V while its nominal operational voltage is 5 V. Operational magnetic flux density interval of the sensor is ± 80 mT (± 800 G) and it can operate at temperatures between - 40ºC and + 150ºC [14].

There are two important criteria for the selection of the coil at which the Hall-effect sensor will be placed. These are permeability of the material and length of the coil, respectively. The size of the air gap which will be prepared for the coil is also an important factor for specifying effective permeability as well as for not spoiling the homogeneity of the flux passing through the air gap. Maximum magnetic flux density generated in the air gap should not be greater than the maximum flux density that the sensor can detect [15]. For the application Ferrite coil OF-42206-TC of Magnetics Company is preferred.

Magnetic flux density generated by the primer current at the toroid coil can be calculated as

$$B = \frac{4\ \pi\ 10^{-7}\ \mu_i\ N\ I}{l_m + l_g\ \mu_i} \tag{1}$$

In this equation, B represents magnetic flux density in T, μ_i represents initial permeability of the coil set by the producing company, $N_P\ I_P$ represents the Magneto Motor Force (MMF) value that is applied to the coil, l_m represents average length of the coil and, l_g represents the length of the air gap.

Calculation of effective permeability of the coil is given below [15-17].

$$\mu_e = \frac{B\, l_m}{N\, I} \tag{2}$$

In order to show sensitivity (S) of the sensor output voltage (V_H) is given as

$$V_H = B\, S \tag{3}$$

By this way, the relation between the current to be measured and the voltage of the sensor is turned out to be:

$$I = \frac{V_H}{S\ \dfrac{4\pi\ 10^{-7}\ \mu_i\ N}{l_m + l_g\ \mu_i}} \tag{4}$$

In this application, the maximum output voltage of the sensor is ± 2.5 V. The initial permeability of the coil is $\mu_i = 3000$, its effective permeability is $\mu_e = 3.738\ 10^{-5}$ H/m, the average length of the coil is $l_m = 54.2$ mm, and the length of air gap is $l_g = 1.8$ mm [16]. According to these parameter values, instant current value is calculated as ±144.75 A. This value is accepted as ±1 pu for convenience and further measured current values are specified according to that value.

3. Mathematical methods

In terms of the mathematical methods, the Fourier transform based approaches are considered as follows.

3.1. Power spectral density

A common approach for extracting the information about the frequency features of a random signal is to transform the signal to the frequency domain by computing the Discrete Fourier Transform (DFT). For a block of data of length N samples, the transform at frequency $m\Delta f$ is given by

$$X(m\Delta f) = \sum_{k=0}^{N-1} x(k\Delta t)\ exp\left[-j2\pi km / N\right] \tag{5}$$

Where Δf is the frequency resolution and Δt is the data-sampling interval. The auto-power spectral density (APSD) of $x(t)$ is estimated as

$$S_{xx}(f) = \frac{1}{N}\left|X(m\Delta f)\right|^2,\ f = \Delta mf \tag{6}$$

The cross power spectral density (CPSD) between $x(t)$ and $y(t)$ is similarly estimated. The statistical accuracy of the estimate in equation [2] increases as the number of data points or the number of blocks of data increases [18-20].

3.2. Short time fourier transform and spectrogram

The Short Time Fourier Transform (STFT) introduced by Gabor in 1946 is useful in presenting the time localization of frequency components of signals. The STFT spectrum is obtained by windowing the signal through a fixed dimension window. The signal may be considered approximately stationary in this window. The window dimension fixed both time and frequency resolutions. To define the STFT, let us consider a signal $x(t)$ with an assumption that it is stationary when it is windowed through a fixed dimension window $g(t)$, centered at time location τ. The Fourier transform of the windowed signal yields the STFT [18-20]

$$STFT\left\{x(t)\right\} \equiv X(\tau, f) = \\ = \int_{-\infty}^{+\infty} x(t)g(t-\tau)\,exp[-j2\pi ft]dt \tag{7}$$

The equation maps the signal into a two-dimensional function in the time-frequency (t, f) plane. The analysis depends on the chosen window $g(t)$. Once the window $g(t)$ is chosen, the STFT resolution is fixed over the entire time-frequency plane. In discrete case, it becomes

$$STFT\left\{x(n)\right\} \equiv X(m, f) = \\ = \sum_{n=-\infty}^{+\infty} x(n)\ g(n-m)\ e^{-jwn} \tag{8}$$

The magnitude squared of the STFT yields the "spectrogram" of the function.

$$Spectrogram\left\{x(t)\right\} \equiv \left|X(\tau, f)\right|^2. \tag{9}$$

4. Measurement system and data acquisition

In this application, to get the data acquisition, Hall Effect sensor type a current transformer is connected to the primary side of the welding machine. This sensor output is sent to the computer system through the PCI hardware, which is multifunction type of Advantech 1716L.

Table
Specific properties of electrical arc welding machine

ELECTRICAL PROPERTIES OF WELDING MACHINES

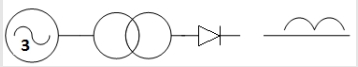

Number of phases: AC, 3

Frequency: 50/60Hz

Primer 100 VA		
110V	220 V	240 V

Seconder 55 V (DC)	
%100	200 A
%35	315 A

In this experiment, the sampling frequency is 200 Hz (sampling time is 0.005 sec.). The analysis of the data from measurement system was performed using the MATLAB. For this purpose, considered measurement and data collection system is shown by (Fig. 2).

Related data used in this study is collected during the welding process of two work pieces as iron material by an electrical arc welding machine (its model is ESAB-LHE 260). Some specific properties of this welter can be given as shown in Table. In this study Metal Active Gas (MAG) welding method is applied. In addition the welding process is made on the ST 37 type material using cored wire with "rutile" basis.

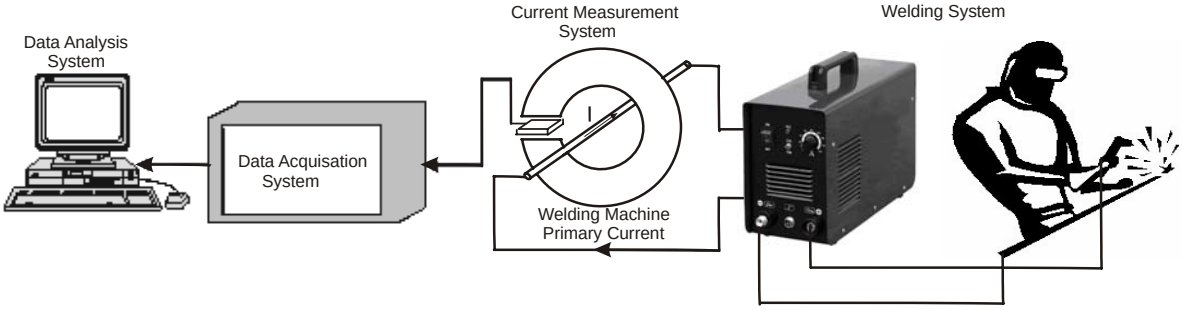

Fig. 2 Measurement system

5. Data analysis and feature extraction

Current variation, which is provided from the measurement system, can be shown by (Fig. 3). Here there are three regions of the current variation. The first part is related to the initial case, before the operation. The second one is transient case and the third one is also due to the operation case of the welding. In this manner (Fig. 3) shows the overall current variation in time domain.

The overall current variation of the welter represents a nonstationary signal. Therefore, one of the suitable mathematical tools to analyze this signal is the short-time Fourier transform.

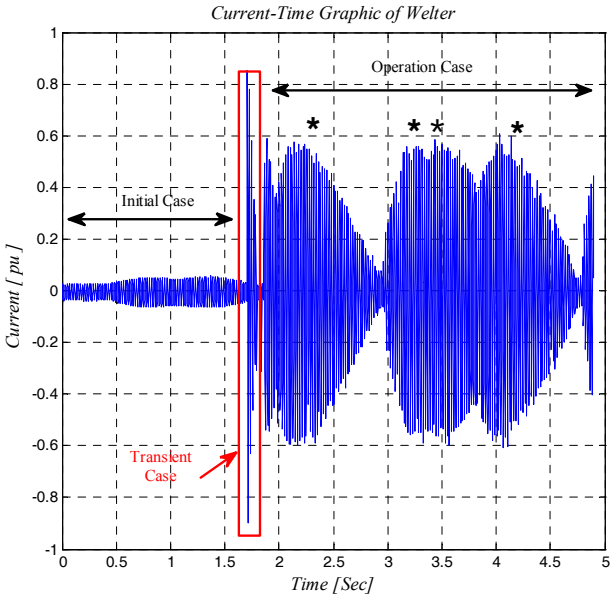

Fig. 3 Overall current variation of the welter (1pu =144.75 A)

In order to get the time-frequency properties of the current variation given above, the spectrogram of the current can be plotted as shown in (Fig. 4) and hence, its frequency changes are easily determined on the time-frequency plane.

According to the results of this determination by the (Fig. 4), fundamental frequency at 50 Hz is dominant and it is appeared overall time. However, there are side band effects at around the fundamental frequency. In this sense, it changes between the 40 and 60 Hz approximately. Also, some effects which come from the initial and transient cases appear on the spectrogram. Here the transient case contains the all frequency band with huge amplitudes between the 0-100 Hz.

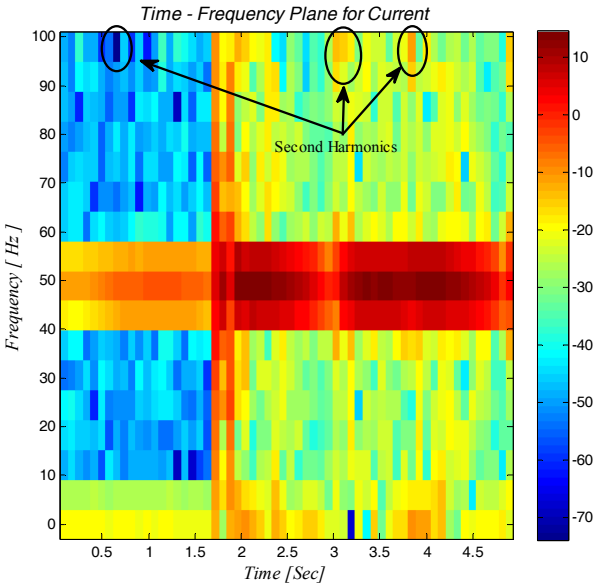

Fig. 4 Spectrogram (Time-Frequency plane) of the current

In this manner, for more sensitive analysis, changing the background color (namely filtering) to indicate the fundamental properties, this spectrogram is reprocessed and then it becomes more sensitive to some frequencies as shown in the (Fig. 5). Here there are four localized regions at the center of the band of 40 - 60 Hz. These are around 50 Hz between 2 and 4.25 seconds. Here the localized regions are related to the maximum variations, which are indicated with symbols (*) on the (Fig. 3), of the current measurement. The bands of 40 - 60 Hz are related to the side band effects. Also, some frequencies before the transient case are obtained at 95 - 100 Hz, 85 - 90 Hz and 10-15 for time interval 0.7-1.5 seconds. The most dominant one of these frequencies is at around the 100 Hz. So, these

harmonic can be interpreted as second harmonic of the fundamental frequency. Also the second harmonics occurred during the operation case.

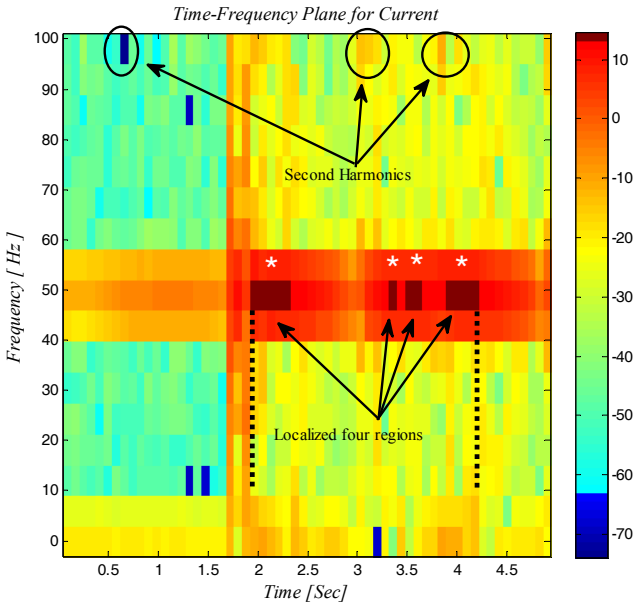

Fig. 5 Filtered Spectrogram (Time-Frequency plane) of the current

To indicate the spectral detail of the band of 40-60 Hz, power spectral density (PSD) function of overall data is considered. Here the PSD approach is suitable for the nonstationary data. Whereas, the current measurement used in this study is a nonstationary. In this sense, the application of the PSD to the nonstationary data does not reflect the time information. However, its results are satisfactory to show the all side bans effect for overall time axis. According to the results of (Fig. 6), the sideband peaks are seen with the differences of 5 Hz around main peak of 50 Hz. Here the first side band effects of the fundamental frequency are seen between the 55 and 45 Hz. This interval can be detected from the (Fig. 5).

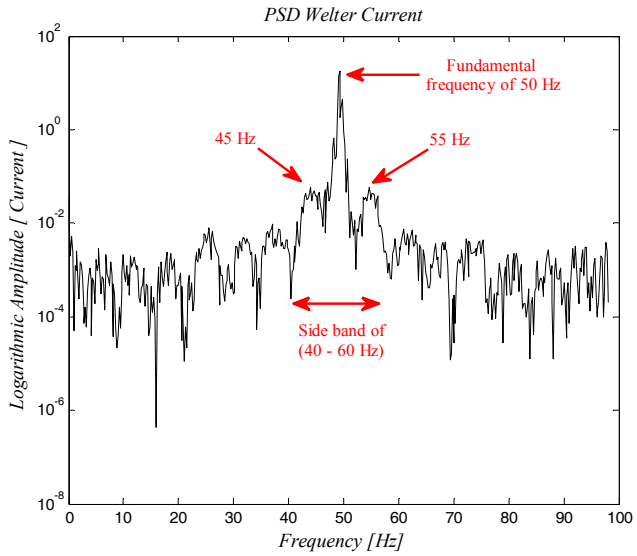

Fig. 6 PSD of current for electric arc welding

Also, this main peak of the PSD variation can be shown by the 3D plot as given in (Fig.7).

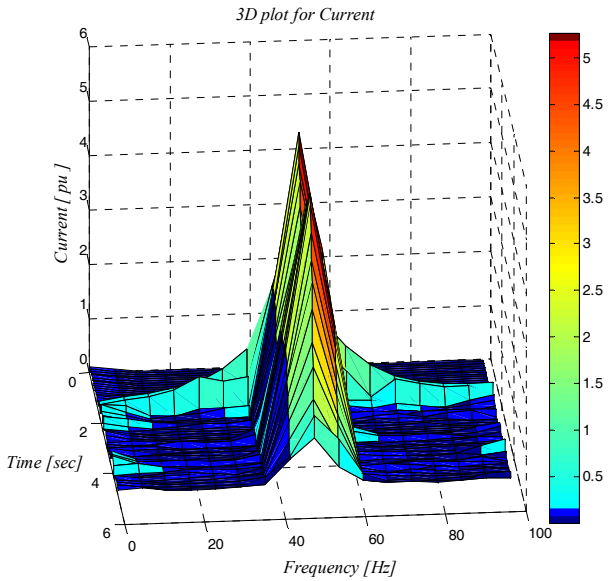

Fig. 7 3D plot for the current

As seen in Fig.7 similar properties like side band of 40-60 Hz and other properties can be shown via this approach too.

6. Concluding remarks

In this study, current changes of an electrical welding machine are taken by means of the measurement system based on Hall effect sensor. Here the sampling frequency is 200 Hz. In terms of the mathematical analysis method, both of the spectrogram and power spectral density approaches are used. According to the analysis results, the obtained findings can be listed as below:

- fundamental frequency at 50 Hz is dominant and it appears overall time that is the stationary characteristics current;
- side band effects like 45 and 55 Hz at around the fundamental frequency are seen with the difference of 5 Hz;
- transient case contains the all frequency band between the 0-100 Hz;
- the second harmonics of the fundamental frequency are determined;
- the fundamental frequency at 50 Hz is strongly localized with four regions between 2 and 4.25 seconds, for the comparisons-so; these regions localized in the frequency domain are related to the maximum points of the current variation in time domain.

All results, which are convenient with the findings above, can be represented by 3D plot given.

Consequently, the fundamental frequency at 50 Hz and its side bands like 45 and 5 Hz are dominant frequency characteristics for this study as well as second harmonic effect. Also, the maximum amplitudes of the fundamental component at 50 Hz appear within very short time between the 2 and 4.25 seconds.

Acknowledgement

Author presents his special thanks to Dr. Gokhan GOKMEN and all people in the Welding Laboratory of

Technology Faculty at Marmara University for their valuable contributions in providing of the data used in this research.

References

1. www.millerwelds.com/interests/instructors/pdf/Electrical_Fundamentals.pdf.
2. **Harry, J.E.** Measurement of electrical parameter of ac arcs- IEEE Transactions on Industry and General Applications, September/October 1969. Vol.IGA-5, No.5, p.624-632.
3. **Hao, X., Song, G.** Spectral analysis of the plasma in low-power laser/arc hybrid welding of magnesium alloy- IEEE Transactions on Plasma Science, Vol.37, Issue.1, 2009, p.76-82.
4. **Ruth, K.** Welding Basics: An Introduction to Practical & Ornamental Welding- Creative Publishing International Inc. Minnesota, ISBN 1-58923-139-2, 2004, p.7-11.
5. **Lancaster, J.F.** The Physics of Welding, Phys. Technology, Vol.15,1984, p.73-79.
6. http://www.ehow.com/about_4661176_electric-welding-machines.html.
7. **Palanco, S., Klassen, M., Skupin, J.** Spectroscopic diagnostics on CW- laser welding plasmas of aluminum alloys, Spectrochim - Acta B, At. Spectrosc., Vol.56, No.6, Jun. 2001, p.651-659.
8. **Karabegović, I, Hrnjica, B.** Simulation of industrial robots for laser welding of load bearing construction. -Mechanika. -Kaunas: Technologija, 2009, Nr.2(76), p.50-54.
9. **Richter-Trummer, V.R., Tavares, S.M.O., Moreira, P. M. G. P., de Castro, P.M.S.T.** Friction stir welding of aluminium allaoys and damage tolerance of integral momolithic structures. -Mechanika. -Kaunas: Technologija, 2008, Nr.5(73), p.50-54.
10. **Mirapeix, J., Cobo A., Conde O.M., Jauregui C., Lopez-Higuera, J.M.,** Real-time arc welding defect detection technique by means of plasma spectrum optical analysis, NDT&E Int. Jul, 2006, Vol.39, No.5, p.356-360.
11. **Azzoni, D., Rüdiger B., Michael F., Harmut G., Hans-Dieter, H., Jürgen K., Andreas, N., Alfred, V.** Isolated Current and Voltage Transducer Characteristic-Applications-Calculations, 1999, p.20-22, LEM Corporate Communications, Genova.
12. **Gilbert, J., Dewey, R.** Application Information, Application Note 27702A, 1-12p, Allegro Microsystem Inc.
13. Amploc Current Sensors, Engineering Reference Book, 2002, p.1-8.
14. Allegro Microsystem Inc., Data Sheet 27501.10B, 3515 and 3516 Ratiometric Linear Hall-Effect Sensors, 2001, p.1-10.
15. Magnetics Division of Spang & Company, Magnetics Cores for Hall Effect Sensors, Technical Bulletin Hed-01, 2001, p.2-6.
16. Magnetics Division of Spang & Company, Design Application Notes, Power Design Section 4, 2006, p.12-13.
17. **Gokmen, G.** Design and Calibration of Electronic Current Transformer, Ph.D. Thesis of Applied Science in Electrical Education, Institute of Pure and Applied Sciences, Marmara University, (in Turkish), 2006, p.42-80.
18. **Vaseghi, S.V.** Advanced Signal Processing and Digital Noise Reduction- John Wiley & Sons Inc, 2000, p.326-328.
19. **Seker, S.** Determination of air-gap eccentricity in electric motors using coherence analysis- IEEE Power Engineering Review, V. 20, N. 7, 2000, p.48-50.
20. **Taskin, S., Seker, S., Karahan, M., Akinci, T.Ç.** Spectral Analysis for Current and Temperature Measurements in Power Cables- Electric Power Components and Systems, Vol.37, Issue.7, April 2009, p.415-426.

T.C. Akinci

SROVĖS SIGNALŲ SUVIRINIMO ĮRENGINYJE ĮVERTINIMAS HOLO JUTIKLIAIS LAIKO IR DAŽNIO METODU

R e z i u m ė

Straipsnyje spektriniu požiūriu analizuojama elektrolankinio suvirinimo įrenginio (EAWM) tiekiama srovė dažnio diapazone. Suvirinimo įrenginio sukuriamos srovės dedamosios nustatomos Holo jutikliu. Tyrimo metu nagrinėti suvirinimo proceso reiškiniai, vykstantys tarp elektrodo ir suvirinamos medžiagos. Šis procesas turi dvi fazes; pereinamąją ir eksploatacinę. Siekiant numatyti suvirinimo įrenginio elgseną šias atvejais, pasiūlytu metodu nustatyta keletas dažnio komponentų. Nustatyta, kad vyraujančioji charakteristika yra išorinio lanko sugeneravimas dažnio diapazone 45 - 55 Hz tai yra su 5 Hz skirtumu į abi puses nuo pagrindinio 50 Hz dažnio. Kita su srove susijusi savybė yra antra pagrindinio dažnio harmonika. Nustatyti ir kiti 45 - 55 Hz diapazone sukuriamo lanko reiškiniai, tačiau jie pasireiškia silpniau. Visos dažnio charakteristikos pateikiamos laiko ir dažnio grafikuose, todėl su laiku ir dažniu susijusios dedamosios lengvai nustatomos.

T.Ç. Akıncı

TIME-FREQUENCY ANALYSIS OF THE CURRENT MEASUREMENTS BY HALL EFFECT SENSORS FOR ELECTRIC ARC WELDING MACHINE

S u m m a r y

In this study, electrical current drawn by an electric arc welding machine (EAWM) is analyzed in frequency domain as a spectral approach. A hall effect sensor is used to get the current drawn by the welter in terms of measurement component. During this study, the stages of the welding process, defined between the material and electrode, are examined. These stages are initial case; transient case and operation case respectively. In this manner, some frequency components are determined for these cases to define the welter behavior. According to the results, side band, which appeared between the 45 - 55 Hz with difference of 5 Hz at around the fundamental frequency 50 Hz, is dominant characteristic. Also, another current related property is the second harmonic of the fundamental frequency. Other band effects are also observed at the outside

of the first band between 45 - 55 Hz however these effects are minor. All frequency characteristics are presented on the time-frequency plane and hence, the time-frequency relationship components are easily determined in this way.

Т.Ц. Акинци

ОЦЕНКА СИГНАЛОВ ТОКА ИСПОЛЬЗУЯ ДАТЧИКИ НОЛЛА В СВАРНОМ УСТРОЙСТВЕ МЕТОДОМ ВРЕМЯ И ЧАСТОТА,

Р е з ю м е

В статье анализируется ток, подаваемый с электродугового сварочного устройства (EAWM) в его частотном диапазоне со спектральной точки зрения. Составляющие тока, создаваемого сварочным устройством, определяются при помощи датчиков Холла. Во время исследований рассматривались явления сварочного процесса, происходящие между электродом и сварочным материалом. Этот процесс состоит из двух фаз: переходной и эксплуатационной. С целью определения поведения сварочного устройства в этих случаях, предложенным методом установлено несколько частотных компонент. Установлено, что определяющей характеристикой является генерирование внешней дуги в частотном диапазоне 45 - 55 Hz, т.е. с разницей 5 Hz в обе стороны по отношению к основной частоте, равной 50 Hz. Другое свойство, связанное с током, это вторая гармоника несущей частоты. Определены и другие свойства дуги, создаваемой в диапазоне 45 - 55 Hz, однако они проявились слабее. Все частотные характеристики представлены в графиках время – частота, поэтому составляющие, связанные с временем и частотой, легко определяются.

Received June 10, 2010
Accepted October 11, 2010

DOI: 10.5755/j02.mech.15954